Hindawi Publishing Corporation
Advances in Materials Science and Engineering
Volume 2014, Article ID 729135, 9 pages
http://dx.doi.org/10.1155/2014/729135

Research Article

Research of Joining Brittle Nonmetallic Materials with an Active Solder

Roman Koleňák and Michal Prach

Faculty of Materials Science and Technology in Trnava, Slovak University of Technology in Bratislava, Paulínska 16, 917 24 Trnava, Slovakia

Correspondence should be addressed to Michal Prach; michal.prach@stuba.sk

Received 29 September 2014; Revised 8 December 2014; Accepted 8 December 2014; Published 22 December 2014

Academic Editor: Dachamir Hotza

This paper deals with soldering high-purity brittle, nonmetallic materials such as SiO_2, Si, and C (graphite). However, these materials exert poor wettability when using tin solder. Therefore, to reduce the wetting angle, an Sn solder alloyed with active Ti element was used. At a soldering temperature of 860°C and 15 min soldering time, the wetting angle on SiO_2 ceramics was 30°, on silicon 42°, and on graphite 52°. All these wetting angles are below 90° and are acceptable for soldering. It has been shown that the bond in all joined materials (SiO_2, Si, and C) was of a diffusion character. New intermetallic products were formed on the boundary with nonmetal, thus allowing bond formation. The shear strength of SiO_2 ceramics attained an average value of 17 MPa.

1. Introduction

For diverse applications, mainly in electronics, we encountered problems with joining nonmetallic and ceramic materials [1–6]. Nowadays soldering offers an alternative method for the fabrication of joints in metallic as well as nonmetallic and ceramic materials.

Fabrication of a sound joint for nonmetallic materials with metallic solder depends on attaining close contact at an atomic distance with the contact surface and whether the metallic solder properly wets the nonmetallic material [7–10]. Wetting nonmetallic materials with metallic solder is a basic precondition for sound joint formation. Moreover, it is also required that the wetting angle in soldering be lower than 90° [11–14]. A sound joint cannot otherwise be assured.

Wettability of nonmetallic materials was the subject of several research works. For example, in [15], the authors studied wetting diamond with pure liquid tin in a shielding atmosphere at temperatures from 500 to 1500°C. Wetting angles of Sn on diamond substrate were within the range from 118 to 160°, which is unacceptable for soldering. Comparative wettability measurements of pure tin were also made by the authors on graphite, where a wetting angle of 155° was measured at a temperature of 1477°C.

Another study [16] dealt with wettability of SiO_2 ceramics with nonactive metals such as Au, Si, and Pb. The measured wetting angle for Au was 143° (1080°C), Si was 87° (1450°C), and Pb attained 120° (727°C). A wetting angle of 87° represents the limit of wettability in soldering. It was found that the bond between solders and substrate is created by Van der Waals forces that represent lower joint strength. However, joint strength is not the subject of this study. Wettability of graphite substrate with liquid Ag-Sn alloy was also studied at temperature intervals from 1000 to 1200°C [17]. The wetting angles were within a range of 125 to 142°.

Thus to ensure the wettability of nonmetallic material and lower the wetting angle, soldering must be done using solder alloyed with an active element [18–22]. Titanium and zirconium are mostly used as the active element [23]. The paper [24] was devoted to the wettability of Si-Al-O-N ceramics with Sn based solders and the addition of different active elements. The Sn-Ti, Sn-Hf, Sn-Zr, and Sn-V soldering alloys were used, achieving wetting angles below 90°. The best results were achieved with Sn-Ti solder, where the wetting angle at temperature 827°C was 25°, which is comparable with wettability on metallic materials. The authors' reason for this fact is that the lower the solubility of Ti in the alloy, the higher the activity of Ti in the liquid alloy.

Table 1: Selected physical properties of ceramic, nonmetallic, and metallic materials [28].

Material/properties	SiO_2	C	Si	AISI 321
Melting point [°C]	1710	3650	1414	1400–1425
Density [g·cm^{-3}]	2.19	2.26	2.33	7.9
Thermal expansivity coefficient [10^{-6} K^{-1}]	0.54	0.6–4.3	2.49	18.0
Young's modulus [GPa]	69	6.9	112.4	190–210
Tensile strength [MPa]	110	28	—	>560

In [25] the silicon substrate was soldered with active solder type Sn-Ag-Ti (Ce). Bond formation between Si and active solder was proven. Bond formation is attributable to the migration of active element on the solder boundary with silicon, resulting in a chemical reaction and formation of an interphase layer containing an oxide of the active element. The strength of the fabricated Si/Si joint was 6.67 MPa.

Wetting and interaction of Sn-Ag-Ti solder on Al_2O_3 and SiC ceramic substrates were studied in [14]. We found that the contact angle of solder on ceramic material is lowered by increased temperature. Better wettability was achieved on SiC ceramics than Al_2O_3 due to a stronger interaction of solder with the surface of SiC ceramics. The wetting angle on Al_2O_3 ceramics was 40° and on SiC ceramics it was almost 0° at 700°C/60 min. It was also found that at 300°C the solder studied became molten but did not wet the ceramics surface. Surface tension forces the droplet to form into an ellipse. By subsequent heating above 700°C, the solder wets both ceramic substrates and the final joint is thus attained.

In [26] the authors joined C/C composite (C/C NS 31 are silicon doped composites: Si 8–10 at. %) with brazing alloy type Ti15Cu15Ni. The presence of Ti guaranteed wetting and adhesion of the substrate. The average shear strength of the joint was 24 MPa.

The authors of study [27] observed the formation of a TiC reaction product on the joint boundary of graphite substrate and brazing alloy type Ti30Zr15Cu10Ni. Active titanium from the brazing alloy created a bond with the graphite substrate. Increased temperature supports Ti diffusion and thus its concentration on the joint boundary, subsequently resulting in bond formation. The formation of an intermetallic compound is attributed to the interdiffusion of metallic elements.

In our work we dealt with soldering high-purity, brittle, nonmetallic materials such as SiO_2, Si, and C. To reduce the wetting angle, Sn solder alloyed with active Ti element was used. From the literature survey it is obvious that the wettability of Sn-Ti based solders and mechanisms of joint formation in soldering SiO_2, Si, and C materials have not yet been the subject of previous studies. The capability of the Sn-Ti alloy to create a sound joint was also studied.

AISI 321 steel was studied to compare results from wettability and shear strength tests. Metallic materials generally exert good wettability and solderability when compared with nonmetallic and ceramic materials. AISI 321 steel served as a reference metallic material.

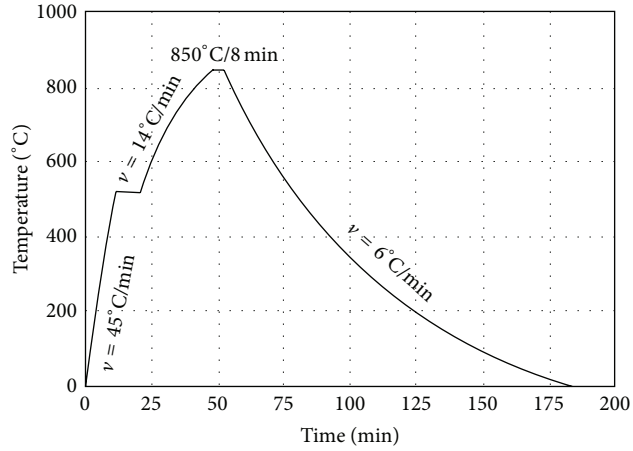

Figure 1: Thermal cycle course of vacuum soldering.

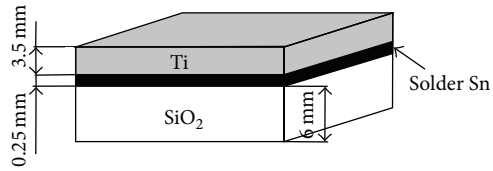

Figure 2: Arrangement of materials at soldering SiO_2.

2. Experimental

Experiments were oriented toward the soldering of high-purity nonmetallic materials such as SiO_2, Si, and C. The SiO_2 ceramic substrate was of 4N5 purity degree (99.995%); graphite and silicon were of 5N purity. Selected properties of substrates used are given in Table 1.

In the first case, nonactive 100Sn solder was used. The purity of this solder was 4N. Solder was enriched during the soldering process by an active element because one of the soldered parts was made of titanium with 99.95% purity.

In the second case, Sn3Ti solder was used for soldering. This solder was prepared by melting Sn with an appropriate amount of Ti at 950°C temperature in a vacuum.

Soldered joints were fabricated in a type PZ 810 electric resistance vacuum furnace in 10^{-2} Pa vacuum. This was applied owing to the high affinity of the active Ti element to oxygen, nitrogen, and hydrogen at higher temperatures. Soldering procedures consisted of inserting the appropriate solder between the joined parts, which were fixed in order to prevent mutual shift. The thermal profile of vacuum furnace soldering is documented in Figure 1. The scheme of experimental specimen is shown in Figure 2.

Specimens were cut after soldering and prepared by a standard metallographic procedure of grinding on SiC emery papers, polishing with diamond pastes with 6, 3, and 1 μm granularity, and chemical polishing with Struers emulsion. The prepared samples were observed in the polished and etched condition by a NEOPHOT 30 type optical microscope. The etched samples were observed on scanning electron

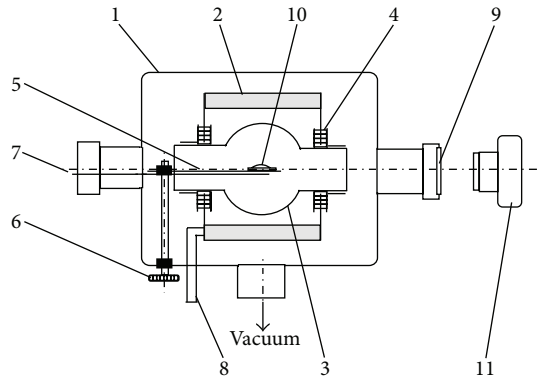

(1) Vacuum bell
(2) Cooling body of the oven
(3) Graphite oven
(4) Fastening ceramic pins
(5) Feeder
(6) Feeder controller
(7) Thermocouple
(8) Inlet and outlet of cooling water
(9) Observation hole for photography
(10) Specimen
(11) Photo camera

FIGURE 3: Schematic representation of apparatus for wettability measurement.

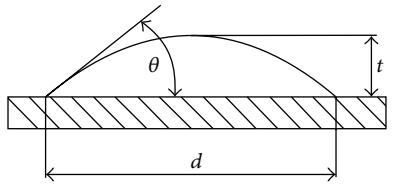

FIGURE 4: Profile of the molten metal drop laying on the support.

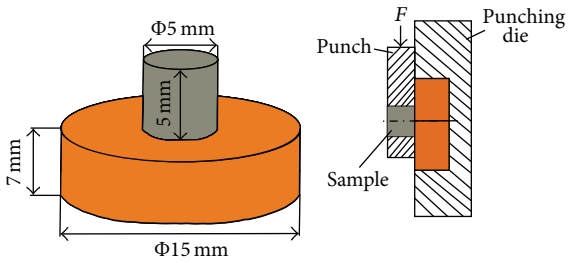

FIGURE 5: Test specimen for shear tests and the scheme of specimen in a jig during the shear test.

microscope type FEI Quanta 200 FEG and JEOL 7600 F with X-ray microanalyser type Microspec WDX-3PC for performing the qualitative and semiquantitative chemical analysis. X-ray diffraction analysis was applied for identification of phase composition by use of Philips PW 1710 equipment.

Wettability measurement of Sn3Ti solder was performed by use of the goniometric method, where the wettability is assessed by the value of wetting angle. The principle of the goniometric method consists of melting of a certain amount of active solder on the appropriate substrate in a vacuum furnace (Figure 3). The registration device is a camera with telephoto lens, by which the specimen is photographed through observation hole of the vacuum bell at preset temperatures. The wetting angle (Θ) is calculated from the parameters of

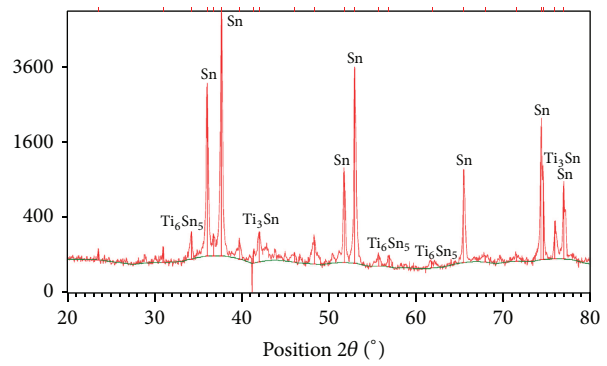

FIGURE 6: Diffraction record of Sn-Ti alloy.

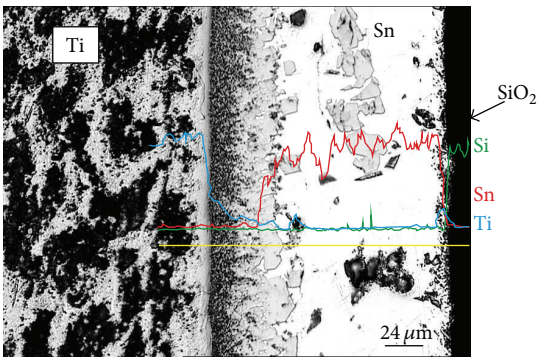

FIGURE 7: Microstructure of Ti/100Sn solder/SiO_2 joint and the concentration profiles of Si, Sn, and Ti elements across the joint boundary.

solder drop (t, d) measured on the snap taken by the camera—Figure 4. The specimen was photographed at set regular time intervals (0, 5, 10, 15, and 20 min) and after assessment, the time dependence of wetting angle size was plotted.

Shear strength was tested on type LabTest 5.250SP1-VM equipment at room temperature. A shearing jig was used for the directional change in axial loading force on the test specimen. This jig ensures a uniform loading of the specimen by shear in the plane of solder and parent metal boundary—Figure 5. The shear gap was selected to 0.1 mm.

3. Experimental Results

3.1. Analysis of SiO_2/100Sn Solder/Ti Substrate Joint. Figure 7 shows the microstructure of the Ti/100Sn solder/SiO_2 joint. Analysis of the chemical composition of soldered joints shows that Ti substrate starts to dissolve in the solder at temperature 770°C and forms a distinct solubility zone in the solder, Figures 7 and 8. The temperature of melting start 770°C was determined by the Sn wettability test on Ti substrate.

The tin matrix of the solder is enriched by 2 to 4 wt. % Ti. EDX and XRD analyses mainly revealed the presence of Ti_6Sn_5 phase and to a lesser extent the Ti_3Sn phase was also observed. Diffraction record is documented in Figure 6.

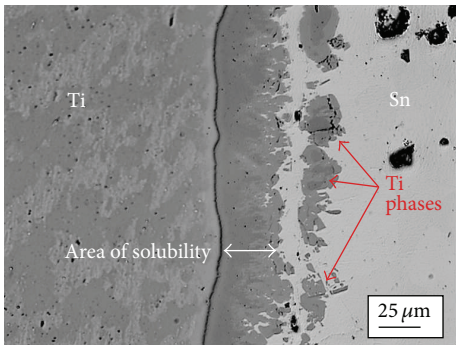

Figure 8: A detailed view on Ti substrate/100Sn solder boundary.

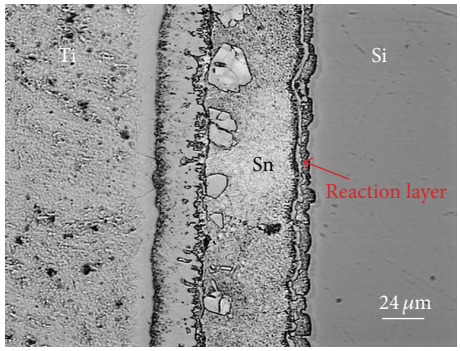

Figure 9: Etched boundary of Ti substrate/100Sn/Si solder.

The active titanium is further distributed to the boundary with ceramic SiO_2 material. We determined its concentration on the solder/SiO_2 boundary (13.6 wt.%). New reaction products are formed by a chemical reaction between active solder and the surface of the ceramic substrate. For example, TiO reaction product was identified there [29]. The reaction product forms the so-called reaction layer and thus ensures the wettability of ceramic material. The bond is of diffusion character.

A detailed view of 100Sn solder/Ti substrate boundary, with a solubility range of titanium in Sn solder, is shown in Figure 8. The band solubility zone of Ti in Sn solder may be observed, which attains an average 37 μm. Ti concentration in the solubility zone is 40 to 59 wt.% Ti, which corresponds to the composition of the Ti_2Sn phase.

3.2. Analysis of Si/100Sn Solder/Ti Substrate Joint. Figure 9 shows the Ti/100Sn solder/Si boundary in etched condition. Using etchant (1.5 mL HF, 3 mL HNO_3, 10 mL H_2O), emphasized titanium, which allows observation of the individual bordered zones in soldered joints (Figure 9).

The reaction layer of the 100Sn solder/Si substrate joint boundary (shown in Figure 10) has an average width ~15 μm. This was formed by the interaction of activated titanium in the solder with the surface of Si substrate. The result of this mutual reaction is a product formed of Ti silicide. This Ti_xSi_y reaction product is responsible for the bond formation

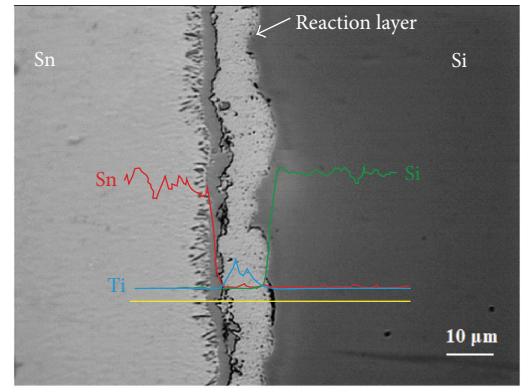

Figure 10: Reaction layer on 100Sn solder/Si substrate boundary and concentration profiles of Si, Sn, and Ti elements across the joint.

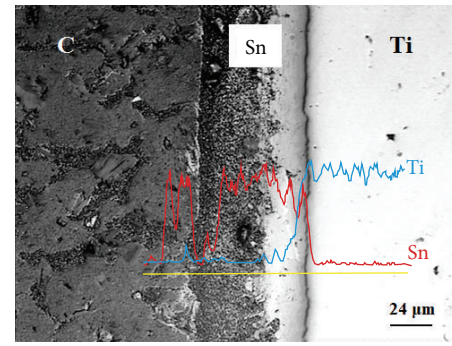

Figure 11: Microstructure of graphite (C)/100Sn solder/Ti substrate boundary and the concentration profiles of Sn and Ti elements across the joint boundary.

between 100Sn solder enriched by Ti and silicon substrate [29].

Concentration of these Si, Sn, and Ti elements across the boundary may be assessed by qualitative chemical analysis—Figure 10. Increased Ti concentrations in the 100Sn solder/Si substrate boundary may be thus observed.

3.3. Analysis of C Graphite/100Sn Solder/Ti Substrate Joint. The microstructure of graphite/100Sn solder/Ti substrate joints after etching is shown in Figure 11. Concentration profiles were determined only for Sn and Ti, since the energy-dispersion analyser on which the chemical analysis was performed does not allow detection of the carbon presence in the sample studied. However, from the Ti concentration profile, it is again evident that Ti shows slightly increased concentration on the solder/graphite boundary.

3.4. Mechanism of Joint Formation. From individual joint analyses, it becomes evident that the joint formation mechanism is identical in all three cases of soldered substrates: SiO_2, Si, and C/Ti. Three basic zones may be identified in the soldered joints (Figure 12):

(i) zone of Ti solubility in Sn solder,

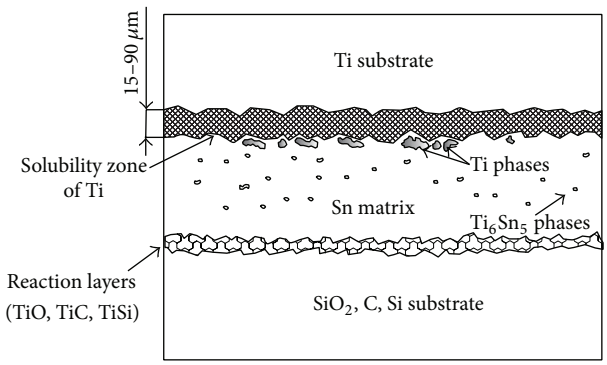

Figure 12: Scheme of individual zones in soldered joint.

(ii) solder matrix formed by tin grains with uniformly distributed Ti_6Sn_5 titanium phase (size of particles of Ti_6Sn_5 titanium phase is 10 to 25 μm),

(iii) reaction layer on the boundary with nonmetallic material.

The individual zones described are of different width. The greater amounts of Ti occurred in the Ti solubility zone in solder (40 to 59 wt.%) and less Ti occurred in solder matrix (2 to 4 wt.%). The titanium content in the reaction layer varies from 2.6 to 12 wt.%. Schematic representations of individual zones in soldered joints are shown in Figure 12.

3.5. Wettability of Sn3Ti Solder. Based on the results, SnTi solder with 3 wt.% Ti was proposed. First of all, its wettability was determined on SiO_2 ceramics and nonmetallic materials (Si and graphite).

Wettability tests on Sn3Ti solder were performed at a temperature of 860°C. Wetting time varied within a range of 5, 10, 15, and 20 min.

In general, wettability on different materials was improved by longer wetting times, with the exception of silicon, where an opposite effect was observed—Figure 13.

On SiO_2 ceramics, at a wetting time of 20 min, a wetting angle of 26° was observed. Observations on graphite at the same wetting time resulted in a 38° wetting angle.

Stainless steel provided a reference material for comparisons of wettability. On stainless steel, using Sn3Ti solder, a wetting angle of 21° was attained at 5 min wetting time. With longer wetting times, the wetting angle on AISI 321 steel improved only slightly—Figure 13.

Wettability tests for Sn3Ti solder were also applied to silicon and graphite. The effects of soldering temperatures on solderability were studied as well. In the case of graphite, the wetting temperature increased from 860°C to 900 and 950°C. Wetting times varied within a range of 5, 10, 15, and 20 min. It was found that the wetting angle on graphite decreases with increased soldering temperatures—Figure 14. After reaching a temperature of 950°C, the wetting angle was 118°. Within 20 min at a temperature 950°C, the wetting angle gradually decreased to 23°, which is comparable with metallic materials.

In determining the wettability of Sn3Ti solder on silicon, an opposite effect was observed—Figure 15. The wetting angle

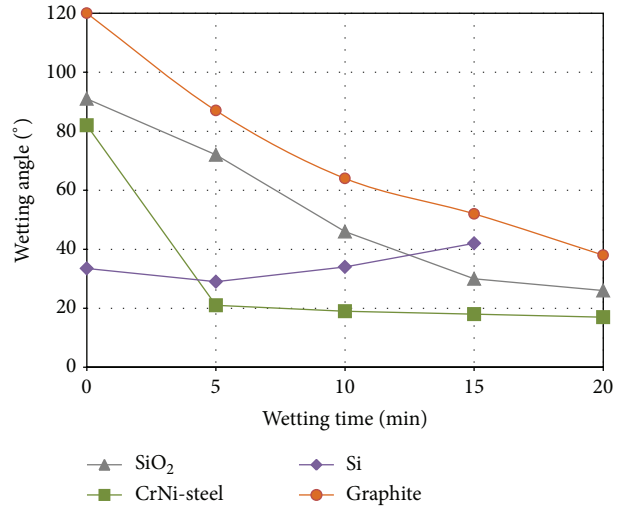

Figure 13: Dependence of wettability of Sn3Ti solder on SiO_2, ceramics, stainless steel type AISI 321, and Si and graphite nonmetals at temperature 860°C.

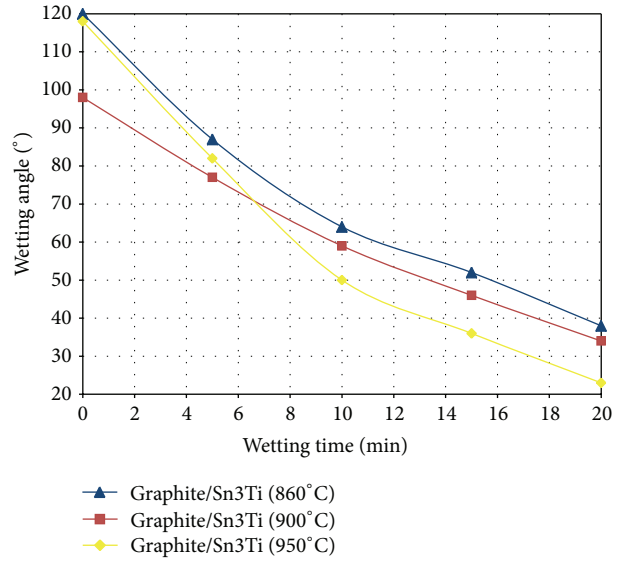

Figure 14: Wettability of Sn3Ti solder on graphite at temperatures 860, 900, and 950°C [21].

at 5 min and 800°C was 19°. During the dwell time at soldering temperature of 15 min, the wetting angle increased to 22°. It became worse at 900°C. At 15 min it increased from an initial 34° to 61°. Analysis has shown that wetting angle is damaged due to the dissolution of silicon substrate and alloying of Sn3Ti solder with silicon [29].

The results of wettability tests of graphite and silicon revealed that, in the case of soldering graphite, it is more advisable to choose higher soldering temperatures and longer dwell times on soldering temperature. On the contrary, in cases of silicon, lower temperatures and shorter soldering times are necessary. In any case, a temperature of 800°C is the lower limit for the thermal activation of titanium in tin solder.

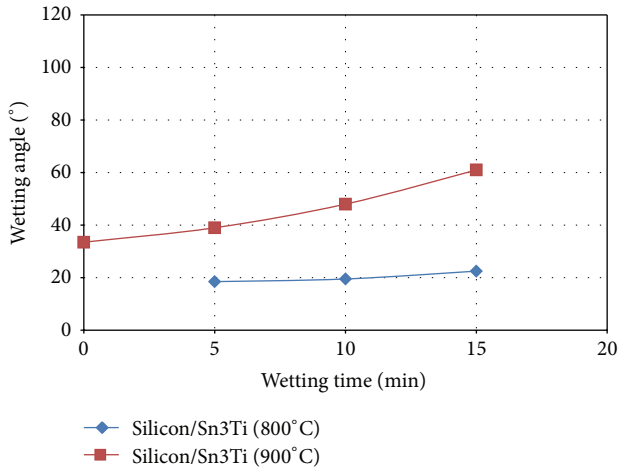

FIGURE 15: Wettability of Sn3Ti solder on silicon at temperatures 800°C and 900°C.

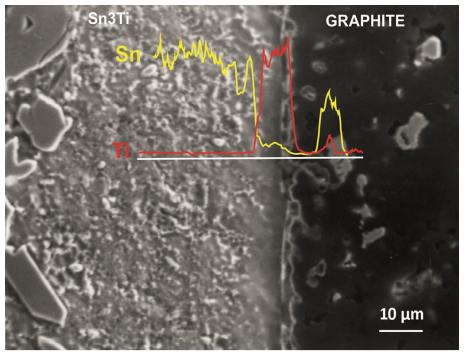

FIGURE 16: Concentration profile of Sn and Ti elements on Sn3Ti solder/graphite boundary [21].

3.6. Analysis of Soldered Joints Fabricated with Sn3Ti Solder. Figure 16 illustrates the microstructure of a graphite/SnTi3 solder joint and the concentration profile of Sn and Ti elements on the graphite/Sn3Ti solder boundary. The amount of active Ti element was determined by EDX analysis. Concentrations of active Ti element in the reaction layer on the graphite/solder boundary varied from 8.98 to 10.11 wt.%. Planar analysis of the graphite/Sn3Ti solder boundary is shown in Figure 17. From this analysis it becomes evident that a maximum concentration of titanium occurred in the reaction layer of the graphite/Sn3Ti solder boundary. The solder is capable of penetrating to the full depth of the graphite substrate. The pores within graphite are filled with tin, with increasing amounts of Ti up to 10 wt.%. This topic about soldering of graphite substrate was discuss detailed in the contribution [21].

Figure 18 illustrates the concentration profile of Si, Sn, and Ti elements on SiO_2/Sn3Ti solder boundaries. The amount of active Ti element was determined by EDX analysis. Concentrations of active Ti element in reaction layers on SiO_2/solder boundaries varied from 4.63 to 5.74 wt.% [30].

Figure 19 illustrates the microstructure of the Sn3Ti/silicon substrate joint. The active Ti reacted, as in previous cases,

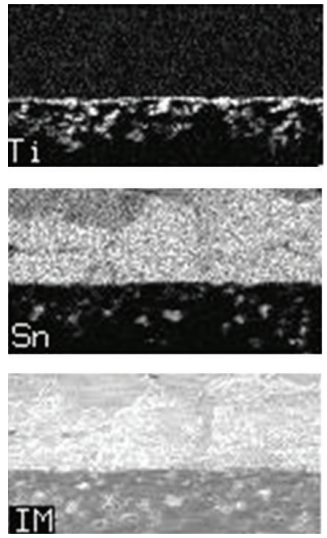

FIGURE 17: Planar distribution of elements on graphite/Sn3Ti solder boundary [21].

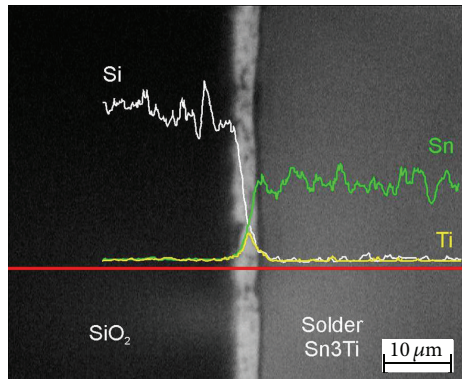

FIGURE 18: Concentration profile of Si, Sn, and Ti elements on SiO_2/Sn3Ti solder boundary [30].

with the surface of silicon substrate at reaction layer formation. The average thickness of this layer was around 4 μm and contained from 5.52 to 7.43 wt.% Ti.

3.7. Shear Strength of Joints. Test specimens of joints were fabricated with Sn3Ti solder by applying findings attained by the measurement of wetting angles. Results of shear strength tests are shown in Figure 20. In cases of soldering SiO_2 ceramics using Sn3Ti solder, an average strength of 17 MPa was achieved.

A higher shear strength of 21 MPa was achieved by soldering stainless steel type AISI 321 joints using Sn3Ti solder.

3.8. Discussion of Results Achieved with Sn3Ti Solder. The results of solder wettability on ceramic and nonmetallic materials such as SiO_2, Si, and C (graphite) proved that Sn solder with Ti content significantly reduces the wetting angle; thus Sn3Ti solder is ideally suitable for practical soldering applications. Contrary to previous studies [15–17], we have achieved wetting angles below 90°. For example, in [16] we

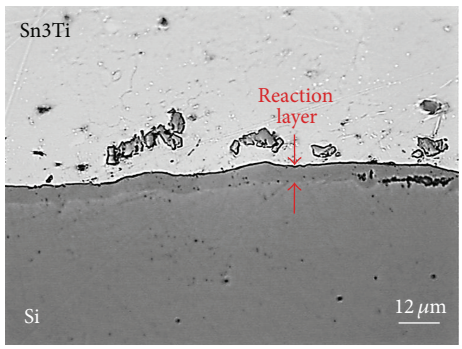

Figure 19: Microstructure of boundary of Si/Sn3Ti joint.

found that the nonactive Au, Si, and Pb metals wet SiO_2 ceramics only with great wetting angles. For Au this was 143° (1080°C), for Si was 87° (1450°C), and for Pb was 120° (727°C). The measured wetting angle for pure tin in study [15] on graphite substrates was 155° at a temperature of 1477°C.

We observed that the wetting angle on SiO_2 ceramics at a temperature of 860°C was 30°, with silicon 42° and graphite 52°. These wetting angles are all well below 90° and are therefore acceptable for soldering. However, tin alloyed with 3 wt.% Ti was used in our case. The wettability achieved is comparable to that observed on metals. For example, the wetting angle achieved on AISI 321 steel, used as reference material, was 21° at 860°C.

Regarding the mechanism of joint formation, in applications of Sn3Ti solder and soldering temperatures above 800°C, a joint formation of diffusion character with the formation of new reaction products was observed. The formation of a new TiC reaction product was also proven in [27], in the case of soldering a graphite substrate with Ti containing solder. To the contrary, in [16] we find that in cases of nonactive metals the bond between solders and substrate created by the Van der Waals forces produces great wetting angles. In [14] it was also proven that, at a temperature of 300°C, solder type Sn-Ag-Ti fails to wet ceramic materials such as Al_2O_3 and SiC. By subsequent heating above 700°C, solder wets the ceramic substrate and the joint can be created.

By comparing results from measurements of shear strength, we also identify the results from similar studies, taking into account that different works make use of different test methods, shape of test specimens, and loading rates at testing. They also use different compositions of solders and soldering parameters. For example, in the case of the application of Sn4Ti solder in [31] in the joint of Ti/Ti metallic material, a shear strength of 16.5 MPa was attained. More studies [25, 32–35] dealt with solder types Sn-Ag-Ti and Sn-Ag-Ti(Ce). They tested metallic, nonmetallic, and ceramic materials.

In study [32], the Al/Al joint showed a shear strength of 15.3 MPa. In [33], the following strengths were achieved by soldering: Cu/Cu (14.3 MPa), ITO/ITO (6.8 MPa), and ITO/Cu (3.4) MPa. Similarly in the study [34] the following shear strength values of joints were attained: Cu/Cu (13.3 MPa) and ZnS-SiO_2/ZnS-SiO_2 (6.5 MPa). The fabricated Si/Si joint [25] demonstrated a shear strength of 6.67 MPa. In our study, similar shear strength results were achieved.

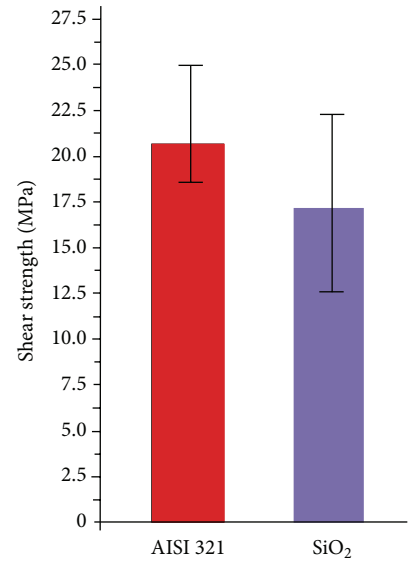

Figure 20: Shear strength of joints fabricated with Sn3Ti solder.

4. Conclusions

The aim of this research is to prove the reaction capacity and wettability of Ti containing solder on selected ceramic and nonmetallic materials to form a strong joint.

The following was discovered on the basis of experiments performed.

(i) Active Ti metal ensured good wetting of ceramic SiO_2 materials as well as nonmetallic materials such as graphite and silicon.

(ii) The wettability of different materials was generally improved by longer wetting times; however, an opposite effect was observed with silicon-wettability deteriorated due to the dissolution of silicon substrate in liquid.

(iii) On SiO_2 ceramics at 20 min wetting time, a wetting angle of 26° was observed. At an identical wetting time, the wetting angle on graphite was 38° and 42° on silicon.

(iv) In soldered joints of ceramic and nonmetallic materials with Ti substrate, three different basic zones may be identified:

  (a) Ti solubility zone in tin solder,
  (b) solder matrix formed of tin grains with a uniformly distributed Ti_6Sn_5 titanium phase,
  (c) reaction layer on the boundary with nonmetallic materials.

(v) The individual zones identified were of varied width. The highest amount of Ti occurred in the Ti solubility zone in the solder (40 to 59 wt.%) and lesser amounts in solder matrix (2 to 4 wt.%). Titanium content in the reaction layer varied from 2.6 to 12 wt.%.

(vi) The mechanism of joint formation in soldering with 100Sn solder is as follows: Ti substrate is dissolved

in Sn solder. Active Ti metal is diffused through the solder matrix up to the boundary of the solder with the ceramic substrate, where it ensures wettability and strong bond formation by its interaction with the surfaces of ceramic and/or nonmetallic materials.

(vii) When soldering SiO_2 ceramics using Sn3Ti solder, an average strength of 17 MPa was achieved. When soldering the joints of stainless steel with the same solder, a higher average shear strength was achieved, even up to 21 MPa.

The performed experiments justified the solution of intricate wettability of brittle ceramic and nonmetallic materials by using active Sn-based solders.

Conflict of Interests

The authors declare that there is no conflict of interests regarding the publication of this paper.

Acknowledgments

This research was supported by APVV-0023-12: research of new soldering alloys for fluxless soldering with application of beam technologies and ultrasound, and VEGA 1/0455/14: research of modified solders for fluxless soldering of metallic and ceramic materials. The authors' thanks belong to Mrs. Bachratá from ÚMMS SAV Bratislava for performing the wettability measurements; Ing. Peter Žúbor, Ph.D., for metallographic analysis; Associate Professor Ing. Maroš Martinkovič, Ph.D., for providing the methodics for shear test measurement; Associate Professor Ing. Martin Kusý, Ph.D., for XRD analysis.

References

[1] A.-P. Xian, "Joining of sialon ceramics by Sn-5 at % Ti based ternary active solders," *Journal of Materials Science*, vol. 32, no. 23, pp. 6387–6393, 1997.

[2] M. Singh, G. N. Morscher, T. P. Shpargel, and R. Asthana, "Active metal brazing of titanium to high-conductivity carbon-based sandwich structures," *Materials Science and Engineering A*, vol. 498, no. 1-2, pp. 31–36, 2008.

[3] H. Ning, Z. Geng, J. Ma, F. Huang, Z. Qian, and Z. Han, "Joining of sapphire and hot pressed Al_2O_3 using $Ag_{70.5}Cu_{27.5}Ti_2$ brazing filler metal," *Ceramics International*, vol. 29, no. 6, pp. 689–694, 2003.

[4] S. Y. Chang, Y. T. Hung, and T. H. Chuang, "Joining alumina to Inconel 600 and UMCo-50 superalloys using an Sn10Ag4Ti active filler metal," *Journal of Materials Engineering and Performance*, vol. 12, no. 2, pp. 123–127, 2003.

[5] W. R. Smith, "Active solder joining of metals ceramics and composites," *Welding Journal*, vol. 10, pp. 30–35, 2001.

[6] R. R. Kapoor and T. W. Eagar, "Tin-based reactive solders for ceramic/metal joints," *Metallurgical Transactions B*, vol. 20, no. 6, pp. 919–924, 1989.

[7] S. Y. Chang, T. H. Chuang, and C. L. Yang, "Low temperature bonding of alumina/alumina and alumina/copper in air using $Sn_{3.5}Ag_4Ti$(Ce,Ga) filler," *Journal of Electronic Materials*, vol. 36, no. 9, pp. 1193–1198, 2007.

[8] R. R. Kapoor and T. W. Eagar, "Tin-based reactive solders for ceramic/metal joints," *Metallurgical Transactions B*, vol. 20, no. 6, pp. 919–924, 1989.

[9] O. M. Kostin, Al. V. Labartkava, and V. A. Martynenko, "Study of the interaction processes of Ti-containing solders with oxide ceramics and Kovar," *Mettallofizika i Noveishie Tekhnologii*, vol. 36, no. 6, pp. 815–827, 2014.

[10] P. Xiao and B. Derby, "Wetting of silicon carbide by chromium containing alloys," *Acta Materialia*, vol. 46, no. 10, pp. 3491–3499, 1998.

[11] H. Manko, *Solders and Soldering*, McGraw-Hill, 4th edition, 2011.

[12] F. Hillen, D. Pickart-Castillo, J. I. Rass, and E. Lugscheider, "Solder alloys and soldering processes for flux-free soldering of difficult to-wet materials," *Welding & Cutting*, vol. 52, no. 8, pp. E162–E165, 2000.

[13] Y. V. Naidich, V. S. Zhuravlev, I. I. Gab et al., "Liquid metal wettability and advanced ceramic brazing," *Journal of the European Ceramic Society*, vol. 28, no. 4, pp. 717–728, 2008.

[14] Y. H. Chai, W. P. Weng, and T. H. Chuang, "Relationship between wettability and interfacial reaction for Sn10Ag4Ti on Al_2O_3 and SiC substrates," *Ceramics International*, vol. 24, no. 4, pp. 273–279, 1998.

[15] K. Nogi, M. Nishikawa, H. Fujii, and S. Hara, "Wettability of diamond by liquid pure tin," *Acta Materialia*, vol. 46, no. 7, pp. 2305–2311, 1998.

[16] R. Sangiorgi, M. L. Muolo, D. Chatain, and N. Eustathopoulos, "Wettability and work of adhesion of nonreactive liquid metals on silica," *Journal of the American Ceramic Society*, vol. 71, no. 9, pp. 742–748, 1988.

[17] Z. Weltsch, A. Lovas, J. Takács, Á. Cziráki, A. Toth, and G. Kaptay, "Measurement and modelling of the wettability of graphite by a silver-tin (Ag-Sn) liquid alloy," *Applied Surface Science*, vol. 268, pp. 52–60, 2013.

[18] R. Koleňák, P. Šebo, M. Provazník, M. Koleňáková, and K. Ulrich, "Shear strength and wettability of active $Sn_{3.5}Ag_4Ti$(Ce, Ga) solder on Al_2O_3 ceramics," *Materials and Design*, vol. 32, no. 7, pp. 3997–4003, 2011.

[19] S. Y. Chang, T. H. Chuang, and C. L. Yang, "Low temperature bonding of alumina/alumina and alumina/copper in air using Sn3.5Ag4Ti(Ce,Ga) filler," *Journal of Electronic Materials*, vol. 36, no. 9, pp. 1193–1198, 2007.

[20] R. Koleňák and M. Prach, "Research of soldering silicon substrate with solders type Sn-Ag-Ti," *Metalurgia International*, vol. 18, no. 8, pp. 260–264, 2013.

[21] R. Koleňák and M. Prach, "Research of joining graphite by use of active solder," *Advanced Materials Research*, vol. 875–877, pp. 1270–1274, 2014.

[22] K. Ferguson, "Active brazing joins titanium-graphite beam target for subatomic particle detection," *Advanced Materials and Processes*, vol. 170, no. 8, pp. 25–27, 2012.

[23] R. Koleňák and M. Prach, "Joining active metals with Al_2O_3 by use of solders," *Advanced Materials Research*, vol. 664, pp. 667–671, 2013.

[24] A.-P. Xian and Z.-Y. Si, "Wetting of tin-based active solder on sialon ceramic," *Journal of Materials Science Letters*, vol. 10, no. 22, pp. 1315–1317, 1991.

[25] C. Peng, M. Chen, and S. Liu, "Die bonding of Silicon and other materials with active solder," in *Proceedings of the International Conference on Electronic Packaging Technology and High Density Packaging*, pp. 275–278, 2010.

[26] P. Appendino, V. Casalegno, M. Ferraris, M. Grattarola, M. Merola, and M. Salvo, "Joining of C/C composites to copper," *Fusion Engineering and Design*, vol. 66–68, pp. 225–229, 2003.

[27] Z. Zhong, Z. Zhou, and C. Ge, "Brazing of doped graphite to Cu using stress relief interlayers," *Journal of Materials Processing Technology*, vol. 209, no. 5, pp. 2662–2670, 2009.

[28] Material Properties Charts, CoorsTek, Inc., http://www.coorstek.com/.

[29] R. Koleňák, *Solderability of metallic and ceramic materials by active solders [Habilitation thesis]*, Slovenská Technická Univerzita, Trnava, Slovakia, 2006.

[30] R. Koleňák and M. Chachula, "Research of joining SiO_2 ceramic material by use of active solder," *Advanced Science Letters*, vol. 19, no. 2, pp. 406–410, 2013.

[31] L. C. Tsao, "Direct active soldering of micro-arc oxidized Ti/Ti joints in air using Sn3.5Ag0.5Cu4Ti(RE) filler," *Materials Science and Engineering A*, vol. 565, pp. 63–71, 2013.

[32] L. C. Tsao, "Interfacial structure and fracture behavior of 6061 Al and MAO-6061 Al direct active soldered with Sn-Ag-Ti active solder," *Materials and Design*, vol. 56, pp. 318–324, 2014.

[33] S. Y. Chang, L. C. Tsao, M. J. Chiang, C. N. Tung, G. H. Pan, and T. H. Chuang, "Active soldering of indium tin oxide (ITO) with Cu in air using an $Sn_{3.5}Ag_4$Ti(Ce, Ga) filler," *Journal of Materials Engineering and Performance*, vol. 12, no. 4, pp. 383–389, 2003.

[34] S. Y. Chang, "Active soldering of ZnS-SiO_2 sputtering targets to copper backing plates using an Sn56Bi4Ti(Ce, Ga) filler," *Materials and Manufacturing Processes*, vol. 21, no. 8, pp. 761–765, 2006.

[35] I. Hlavatý, "Solderability of high-purity aluminium with the lead-free tin solders," in *Proceedings of the 22st International DAAAM Symposium "Intelligent Manufacturing and Automation"*, vol. 22 of *Annals of DAAAM*, pp. 818–819, Vienna, Austria, 2011.